

# ELECTRICAL RESISTIVITY AND MAGNETORESISTANCE PROPERTIES OF CATION A-SITE SUBSTITUTION IN La<sub>0.8-x</sub>Ag<sub>x</sub>Ca<sub>0.2</sub>MnO<sub>3</sub> (x = 0.1 and 0.15)

# Dicky Rezky Munazat<sup>1,4</sup>, Budhy Kurniawan<sup>\*1</sup>, Rina Kamila<sup>2</sup>, Maykel Manawan<sup>3,4</sup> and Agung Imaduddin<sup>4</sup>

<sup>1</sup> Department of Physics, Faculty of Mathematics and Natural Sciences (FMIPA), Universitas Indonesia, Depok 16424, Indonesia

National Research and Innovation Agency (BRIN), South Tangerang 15314, Banten, Indonesia
 <sup>3</sup>Fakultas Teknologi Pertahanan, Universitas Pertahanan Indonesia, Bogor 16810, Indonesia
 <sup>4</sup>Research Center for Advanced Material, National Research and Innovation Agency (BRIN), South Tangerang 15314, Banten, Indonesia
 \*budhy.kurniawan@sci.ui.ac.id

Received 2023-11-03, Revised 2024-10-18, Accepted 2025-08-05, Available Online 2025-10-01, Published Regularly October 2025

#### **ABSTRACT**

In this study, we investigated the electrical resistivity and magnetoresistance of polycrystalline La<sub>0.8-x</sub>Ag<sub>x</sub>Ca<sub>0.2</sub>MnO<sub>3</sub> (x = 0.1 and 0.15) samples. All samples exhibited metallic behavior, as evidenced by the resistivity data measured in the temperature range of 9–285 K. As the Ag concentration increased, the resistivity decreased throughout the entire temperature range. Increasing the silver ion concentration improves the double exchange interaction (DE) between Mn<sup>3+</sup> and Mn<sup>4+</sup>, which is responsible for the gradual decrease in resistivity. The electrical transport properties are well described by a theory based on the grain boundary factor, electron-electron interaction, and Kondolike spin-dependent scattering mechanisms. Both samples exhibited low-field magnetoresistance (LFMR) at low temperatures. The maximum magnetoresistance values for both samples were observed at 15 K, with values of -23.16% and -25.17% for x = 0.10 and 0.15, respectively.

Keywords: Double exchange; Electrical transport; Magnetoresistance; Perovskite Manganite; Silver substitution

## INTRODUCTION

Mixed-valence Lanthanum Manganite of the form La<sub>1-x</sub>A<sub>x</sub>MnO<sub>3</sub>, where A represents divalent alkaline-earth or monovalent alkali-metal elements, has received great attention owing to its unique electrical transport properties and colossal magnetoresistance effect (CMR) [1], [1], [2], [3]. The unique properties of these materials have attracted significant scientific and technological attention. These materials can be applied to spintronic devices, such as magnetic sensors, magnetic storage, and uncooled infrared bolometers [4], [5]. Generally, the double-exchange interaction theory has been used to explain the physical properties of these compounds. The substitution level (x) of La ions strongly influences the Mn<sup>3+</sup>/Mn<sup>4+</sup> ratio. The partial substitution changes in the average ionic radius ( $< r_A >$ ) and cation mismatch ( $\sigma^2$ ) distort the MnO<sub>6</sub> octahedron, which corresponds to the double-exchange interaction of the magnetic coupling Mn<sup>3+</sup>-O-Mn<sup>4+</sup> [1].

The electrical properties of mixed-valence manganites can be sufficiently described by double-exchange interaction theory. Several researchers have proposed theoretical models based on grain boundaries (GBs), electron-electron interactions, electron-phonon interactions, electron-magnon interactions, Kondo-like spin dependence, and intergranular spin-polarized tunneling [5], [6]

We have previously studied the effect of silver (Ag<sup>+</sup>) substitution on the structural and electrical properties and magnetoresistance of La<sub>0.8-x</sub>Ag<sub>x</sub>Ca<sub>0.2</sub>MnO<sub>3</sub> (x=0 and 0.05) <sup>[7], [8]</sup>. It was observed that the resistivity decreased with Ag substitution compared to that of the parent compound. To continue with the previous investigation, in this study, we increased the silver concentration by introducing x=0.1 and x=0.15 into La<sub>0.8-x</sub>Ag<sub>x</sub>Ca<sub>0.2</sub>MnO<sub>3</sub>. The electrical resistivity and magnetoresistance of both samples were investigated. Polycrystalline samples of La<sub>0.8-x</sub>Ag<sub>x</sub>Ca<sub>0.2</sub>MnO<sub>3</sub> (x=0.1 and 0.15) were successfully synthesized using the sol-gel method, as described in our previous study <sup>[8]</sup>. It was observed that the material crystallizes in an orthorhombic structure for x=0.1 and a rhombohedral structure for x=0.15 <sup>[8]</sup>. In this study, we also explored and discussed the correlation between the structure, morphology, and transport mechanisms of both samples.

#### **METHOD**

Polycrystalline La<sub>0.8-x</sub>Ag<sub>x</sub>Ca<sub>0.2</sub>MnO<sub>3</sub> (x = 0.1 and 0.15) was prepared using the sol-gel method, with the synthesis method described in a previous work <sup>[8]</sup>. The samples were prepared using a sol-gel method. The starting materials for the synthesis were La<sub>2</sub>O<sub>3</sub>, AgNO<sub>3</sub>, Ca(NO<sub>3</sub>)<sub>2</sub>·4H<sub>2</sub>O, and Mn(NO<sub>3</sub>)<sub>2</sub>·4H<sub>2</sub>O. Citric acid (C<sub>6</sub>H<sub>8</sub>O<sub>7</sub>·H<sub>2</sub>O) was added as a catalyst, and HNO<sub>3</sub> (ammonia solution) was used to neutralize the pH of the solution. All materials were mixed based on stoichiometric calculations and stirred continuously at a temperature–75-80 °C until a viscous gel was formed. The resulting viscous gel underwent three heating stages: dehydration at 120 °C for 3 h, calcination at 550 °C for 5 h, and sintering into pellets at 900 °C for 24 hours. The Surface microstructures and morphologies were examined using a scanning electron microscope (SEM). Temperature-dependent resistivity and magnetoresistance measurements were conducted using a standard DC four-probe method over a temperature range of 9–285 K with a Cryogenic Magnetometer (Oxford Teslatron instrument).

#### **RESULTS AND DISCUSSION**

# 3.1. Morphology.

Figure 1 shows the SEM images of both samples. The grain size of the sample was identified using 20.000 magnification. The average grain sizes were determined using the ImageJ software. Grain size distribution histograms were analyzed by fitting them with a normal distribution function to ensure normal distribution. The grain size for x = 0.1 was smaller than that for x = 0.15.

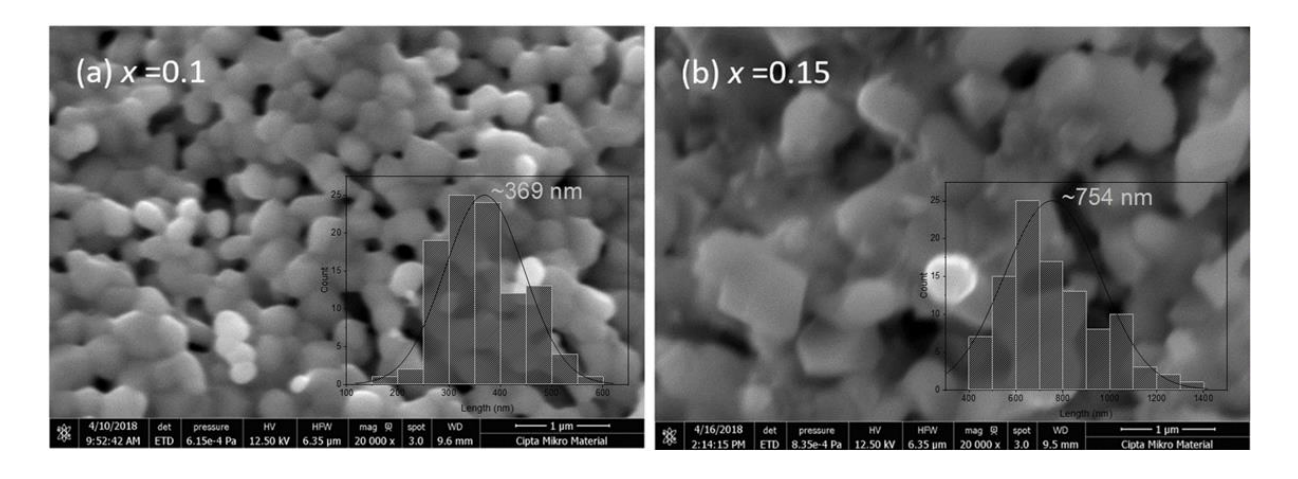


**Figure 1.** SEM images of  $La_{0.8-x}Ag_xCa_{0.2}MnO_3$  (a) x = 0.1 and (b) x = 0.15. Inset grain size distribution histograms

# 3.2. Electrical Transport

Our previous work also showed that Ag substitution decreased the resistivity <sup>[7]</sup>. The overall resistivity decreases with increasing concentration of the silver substitution value, as shown in Figure 2. The temperature-dependent resistivity of both samples is shown in the inset of Figure 2. Metallic behavior was observed at all temperatures for both samples. The resistivity of the sample decreased with increasing Ag concentration.

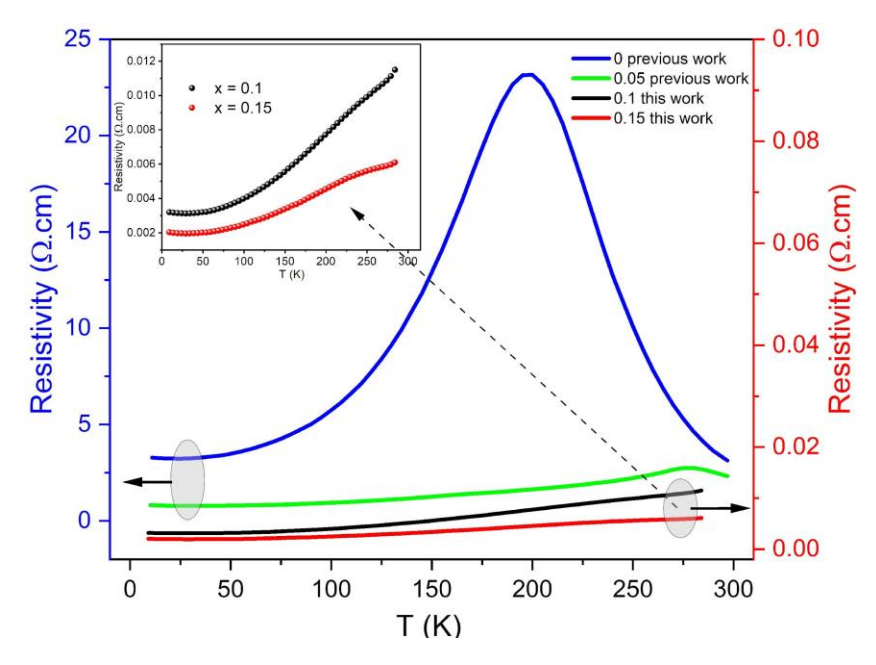


**Figure 2.** Temperature-dependent of resistivity for  $La_{0.8-x}Ag_xCa_{0.2}MnO_3$  (x = 0-0.15) compared with our previous work

Partial A-site cation substitution with Ag ions affects the double-exchange interactions, resulting in resistivity changes <sup>[9]</sup>. Based on this chemical formula, the ionic stability of this compound is given by La<sub>0.8-x</sub>Ag<sub>x</sub>Ca<sub>0.2</sub>Mn<sup>3+</sup><sub>(1-(0.2+x))</sub>Mn<sup>4+</sup><sub>(0.2+x)</sub>O<sub>3</sub>. When the concentration of silver (Ag<sup>+</sup>) ions increases, the number of Mn<sup>4+</sup> ions increases, causing an increase in the Mn<sup>3+</sup>-O-Mn<sup>4+</sup> coupling ratio, which also improves the double-exchange interaction of the sample <sup>[10]</sup>. Silver substitution also changes the  $< r_A >$  and  $\sigma^2$  in the structural,  $< r_A > = 1.215$  and 1.218

Å and  $\sigma^2 = 6.68 \times 10^{-4}$  and  $8.67 \times 10^{-4}$  for x = 0.10 and 0.15, respectively. This change creates a distortion of the MnO<sub>6</sub> octahedron, which corresponds to the double exchange interaction of the magnetic coupling Mn<sup>3+</sup>-O-Mn<sup>4+[1]</sup>. Based on our previous study, Ag substitution increases the average bond angle (<Mn-O-Mn>) while reducing the average Mn-O bond length (<Mn-O>) in MnO<sub>6</sub> octahedra

This affects the electronic bandwidth, which can be approximated by the following equation<sup>[11]</sup>:

$$W = \frac{\cos\frac{1}{2}(\pi - \langle Mn - O - Mn \rangle)}{d_{\langle Mn - O \rangle}^{3.5}}$$
(1)

The estimated values of the bandwidth W are 0.933 and 0.953 for x = 0.1 and 0.15, respectively. This is in good agreement with the fact that for x = 0.15, the resistivity is lower than that for x = 0.1. The greater the W value, the easier the double-exchange interaction because the <Mn-O> value is smaller, and the <Mn-O-Mn> value is larger. Electrons are more easily transferred from Mn<sup>3+</sup> to Mn<sup>4+</sup> via O<sup>2-[11]</sup>. Resistivity is also influenced by extrinsic factors such as grain boundaries. As shown in Figure 1, the grain size for x = 0.1 is smaller than that for x = 0.15. This is in good agreement with the resistivity data. The increased grain size reduces the number of grain boundaries and grain boundary scattering, which improves the conductivity of the samples, thus decreasing the resistivity [12].

A theoretical model was used to further understand the electrical transport behavior of the samples. Generally, the temperature dependence of the resistivity in the metallic behavior of the mixed-valence manganite-based compound can be expressed by the following equations [13].

$$\rho(T) = \rho_0 + \rho_e T^{\frac{1}{2}} - \rho_s \ln T + \rho_p T^5 + \rho_2 T^2 + \rho_{9/2} T^{9/2}$$
 (2)

The  $\rho_0$  represents the residual resistivity attributed to grain boundaries and temperature-independent processes, such as domain wall effect,  $\rho_e\,T^{1/2}$  arises from electron-electron interactions,  $\rho_s \ln T$  corresponds to Kondo-like spin-dependent scattering,  $\rho_p\,T^5$  is a consequence of electron-phonon interactions,  $\rho_2\,T^2$  is associated electron-electron scattering, and  $\rho_{9/2}\,T^{9/2}$  is a combination of electron, magnon, and phonon scattering processes. Figure 3 shows the temperature-dependent resistivity fitting using Equation 2. The fitting parameters are listed in Table 1.

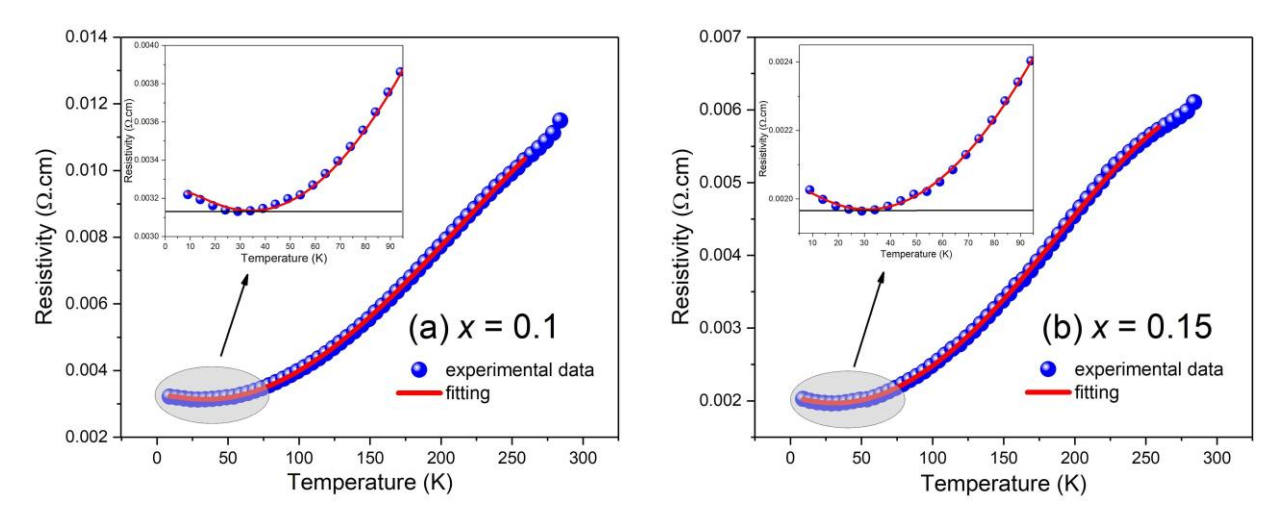


**Figure 3.** (a) Temperature dependence of the resistivity of  $La_{0.8-x}Ag_xCa_{0.2}MnO_3$  (x = 0.1 and 0.15) and (b) comparison with our previous work (Munazat et al., 2019).

**Table 1.** Fitting resistivity obtained from resistivity data of metallic region for  $La_{0.8-x}Ag_xCa_{0.2}MnO_3$  (x = 0.1 and 0.15).

Resistivity Parameter	Silver Concentration $(x)$	
	0.1	0.15
$\rho_0^{}\left(\Omega.cm\right)$	0.00325	0. 00208
$ \rho_e \left( \frac{\Omega \cdot cm}{K^{1/2}} \right) $	-2.717 x 10 <sup>-4</sup>	-1.079 x 10 <sup>-4</sup>
$\rho_s (\Omega.cm)$	-3.551 x 10 <sup>-4</sup>	-1.149 x 10 <sup>-4</sup>
$\rho_p \left( \frac{\Omega.  cm}{K^5} \right)$	2.503 x 10 <sup>-15</sup>	-1.247 x 10 <sup>-15</sup>
$ \rho_2 \left( \frac{\Omega \cdot cm}{K^2} \right) $	1.884 x 10 <sup>-7</sup>	9.663 x 10 <sup>-7</sup>
$\rho_{\frac{9}{2}}(\frac{\Omega.cm}{K^{9/2}})$	-8.369 x 10 <sup>-13</sup>	-3.501 x 10 <sup>-15</sup>
$R^{2}(\%)$	99.98	99.98

Based on Table 1, the  $\rho_0$ ,  $\rho_e$ , and  $\rho_s$  parameters have a significant values compared to the other parameters. The grain boundary factor, electron-electron interaction, and Kondo-like spin-dependent scattering mechanisms are strongly correlated in the transport mechanism in both samples. Based on the SEM image in Figure 1, the grain size for x=0.1 is lower than that for x=0.15. This is in good agreement with the  $\rho_0$  value. The value of  $\rho_0$  for x=0.1 is higher than that for x=0.15, suggesting an enhancement in the residual resistivity arising from vacancies, grain boundaries, and domain walls [2].

The Kondo-like spin-dependent scattering mechanisms can be evaluated from the inset of Figure 3, at low temperatures. The figure shows that in the upturn, the resistivity tends to increase as the temperature decreases after reaching its minimum value of  $0.00323~\Omega$ . cm at T = 31.7 K for x=0.1 and  $0.00196~\Omega$ . cm at T = 29 K for x=0.15. This minimum resistivity occurs as an alternative electron scattering process was taking place. The presence of a magnetic

moment in manganese (Mn) within La<sub>0.8-x</sub>Ag<sub>x</sub>Ca<sub>0.2</sub>MnO<sub>3</sub> (x = 0.1 and 0.15) leads to a scattering process that involves a transient exchange of spin states between conduction electrons and magnetic impurities. The Kondo effect ( $\rho_s$ ) parameter for x = 0.15 was greater than that for x = 0.1. This corresponds to the electronic bandwidth, indicating the ease with which electrons can interact. Kondo applied a model for scattering involving a magnetic impurity interacting with the spins of conducting electrons using perturbation theory. He found that the second-order term in the calculation could become larger than the first, leading to a logarithmic increase in the resistance of a metal as the temperature decreased [14].

# 3.3. Magnetoresistance

The magnetic field dependence of the magnetoresistance measured at 15, 150, 200, and 285 K for both samples is presented in Figure 4. The magnetoresistance ratio is defined as

$$MR\% = \frac{\rho(H) - \rho(0)}{\rho(0)}$$
 (3)

where  $\rho(H)$  and  $\rho(0)$  represent the resistivity under applied magnetic field and zero field, respectively. As shown in Figure 4, the maximum MR value for both samples under an applied field of 1 T was obtained at 15 K, - 23.16% for x = 0.10 and -25.17% for x = 0.15.

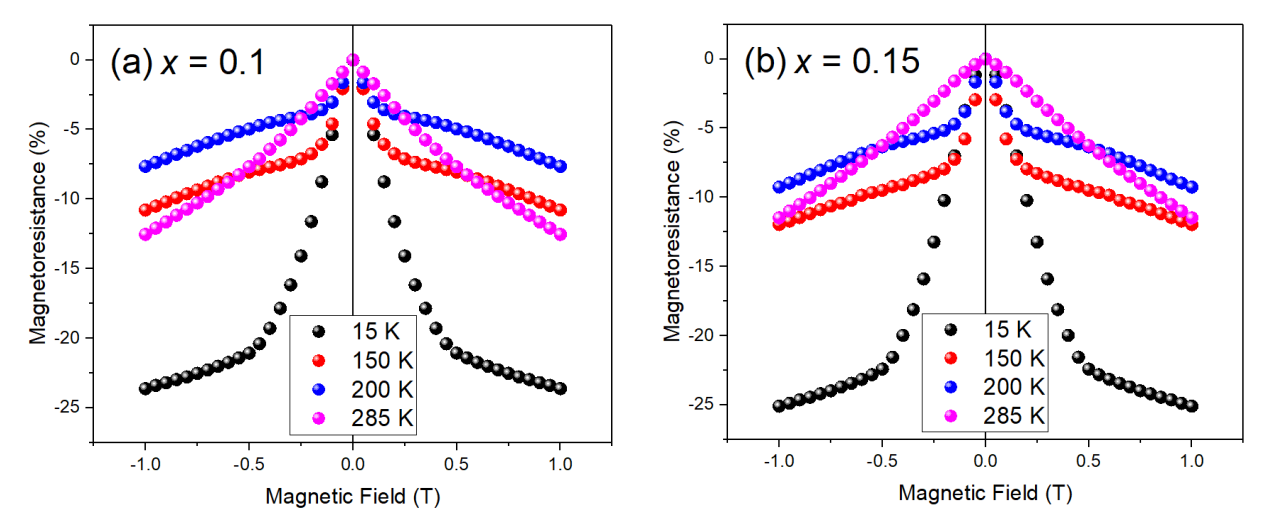


**Figure 4.** Magnetoresistance ratio at various temperatures for  $La_{0.8-x}Ag_xCa_{0.2}MnO_3$  (a) x = 0.1 and (b) x = 0.15.

At low temperatures, both samples exhibited low-field magnetoresistance (LFMR). In the lower magnetic field (H < 0.5 T), the magnetoresistance exhibits a sharply increasing curve at low magnetic fields, transitioning to a linear curve as the magnetic field strength increases. This behavior of magnetoresistance can be considering intergranular spin-polarized electron tunneling near the grain boundaries [15].

#### CONCLUSION

In summary, we conducted a study on the electrical transport and magnetoresistance properties of  $La_{0.8-x}Ag_xCa_{0.2}MnO_3$  compounds with x values of 0.1 and 0.15. Both samples exhibited metallic behavior across all temperature ranges. We observed that the substitution of silver (Ag+) leads to a decrease in the overall resistivity compared to that of the parental compound. Our calculations, based on a theoretical model, revealed that the transport mechanism in both

samples was strongly influenced by electron-electron interactions and grain boundaries. As the concentration of substituted silver ions increased, the number of  $Mn^{4+}$  ions also increased. This resulted in an increased ratio of  $Mn^{3+}$ -O- $Mn^{4+}$ , leading to heightened double-exchange interactions and electronic bandwidth. Consequently, the resistivity of the sample decreased. The electrical transport behavior is also influenced by the residual resistivity from the grain boundaries and exhibits a Kondo-like effect. Both samples exhibited Low-Field Magnetoresistance (LFMR) at low temperatures. Notably, the maximum magnetoresistance values for both samples were obtained at 15 K, -23.16% and -25.17% for x = 0.10 and 0.15, respectively.

## **ACKNOWLEDGMENTS**

This work was funded by a grant from the Ministry of Research and Technology/National Research and Innovation Agency of Indonesia (Kemenristek/BRIN) with PDUPT 2021 grant [NKB-160/UN2.RST/HKP.05.00/2021].

#### **REFERENCES**

- [1] Ah. Dhahri, M. Jemmali, E. Dhahri, and E. K. Hlil, "Electrical transport and giant magnetoresistance in La<sub>0.75</sub> Sr<sub>0.25</sub> Mn<sub>1-x</sub> Cr<sub>x</sub> O<sub>3</sub> (0.15, 0.20 and 0.25) manganite oxide," *Dalton Trans.*, vol. 44, no. 12, pp. 5620–5627, 2015, doi: 10.1039/C4DT03662J.
- [2] O. Vitayaya *et al.*, "Enhanced magnetoresistance properties of K-site deficient La<sub>0.85</sub> K<sub>0.1</sub> □<sub>0.05</sub> MnO<sub>3</sub> manganites synthesized *via* sol–gel, wet-mixing, and solid-state reaction methods," *RSC Adv.*, vol. 14, no. 52, pp. 38615–38633, 2024, doi: 10.1039/D4RA07105K.
- [3] S. Zhang *et al.*, "Effect of Na-doping on structural, electrical, and magnetoresistive properties of La0.7(Ag0.3-Na)0.3MnO3 polycrystalline ceramics," *Ceram. Int.*, vol. 46, no. 1, pp. 584–591, Jan. 2020, doi: 10.1016/j.ceramint.2019.09.006.
- [4] H. Li *et al.*, "A-site mixed-valence co-doping to optimize room-temperature TCR of polycrystalline La0.8K0.04Ca0.16-Sr MnO3 ceramics," *Ceram. Int.*, vol. 46, no. 13, pp. 20640–20651, Sept. 2020, doi: 10.1016/j.ceramint.2020.04.109.
- [5] H. Li *et al.*, "Electrical transport properties of La0.845Sr0.155MnO3:K (0 ≤ x ≤ 0.2) composites," *J. Alloys Compd.*, vol. 810, p. 151908, Nov. 2019, doi: 10.1016/j.jallcom.2019.151908.
- [6] A. Zahrin, N. Ibrahim, and Z. Mohamed, "Effects of Li substitution on structural, magnetic properties and electroresistance behaviour in La0.8Na0.2-Li MnO3 monovalent-doped manganite," *Mater. Sci. Eng. B*, vol. 295, p. 116613, Sept. 2023, doi: 10.1016/j.mseb.2023.116613.
- [7] D. R. Munazat, B. Kurniawan, A. Imaddudin, R. Kamila, and D. S. Razaq, "Effect of Silver Substitution on Electrical Transport and Magnetoresistance of La<sub>0.8</sub> Ca<sub>0.2</sub> MnO<sub>3</sub>," *IOP Conf. Ser. Mater. Sci. Eng.*, vol. 546, no. 4, p. 042025, June 2019, doi: 10.1088/1757-899X/546/4/042025.
- [8] R. Kamila and B. Kurniawan, "Influence of silver (Ag) doping on a crystal structure of La<sub>0.7</sub> Ag<sub>0.1</sub> Ca<sub>0.2</sub> MnO<sub>3</sub> and La<sub>0.65</sub> Ag<sub>0.15</sub> Ca<sub>0.2</sub> MnO<sub>3</sub> manganites synthesized by sol-gel method," *J. Phys. Conf. Ser.*, vol. 1170, p. 012065, Mar. 2019, doi: 10.1088/1742-6596/1170/1/012065.
- [9] A. Modi, D. K. Pandey, S. Bhattacharya, S. Mukherjee, G. S. Okram, and N. K. Gaur, "Improved temperature coefficient of resistance and transport properties of Nd0.7Sr0.3–xAxMnO3 (A = Ag, Na, K: x = 0 & 0.1) manganites," *J. Mater. Sci. Mater. Electron.*, vol. 32, no. 18, pp. 23134–23145, Sept. 2021, doi: 10.1007/s10854-021-06799-1.
- [10] X. Zhu *et al.*, "Co-optimization of Ag and K doping to regulate room-temperature coefficient of resistivity of La0.7Ag0.3-K MnO3 films," *Appl. Surf. Sci.*, vol. 630, p. 157511, Sept. 2023, doi: 10.1016/j.apsusc.2023.157511.
- [11] A. N. Ulyanov, A. V. Vasiliev, E. A. Eremina, O. A. Shlyakhtin, S. V. Savilov, and E. A. Goodilin, "Phenomenological description of doped manganites. Electron bandwidth, crystal local structure

- and Curie temperature," *Ceram. Int.*, vol. 44, no. 18, pp. 22297–22300, Dec. 2018, doi: 10.1016/j.ceramint.2018.08.354.
- [12] Y. Liu, T. Sun, G. Dong, S. Zhang, and X. Liu, "Electrical conduction in La0.85Sr0.15MnO3:Ag  $(0 \le x \le 0.5)$  ceramics with large room-temperature TCR," *Ceram. Int.*, vol. 45, no. 18, pp. 24070–24077, Dec. 2019, doi: 10.1016/j.ceramint.2019.08.113.
- [13] Ah. Dhahri, M. Jemmali, K. Taibi, E. Dhahri, and E. K. Hlil, "Structural, magnetic and magnetocaloric properties of La0.7Ca0.2Sr0.1Mn1–Cr O3 compounds with x= 0, 0.05 and 0.1," *J. Alloys Compd.*, vol. 618, pp. 488–496, Jan. 2015, doi: 10.1016/j.jallcom.2014.08.117.
- [14] J. Kondo, "Resistance Minimum in Dilute Magnetic Alloys," *Prog. Theor. Phys.*, vol. 32, no. 1, pp. 37–49, July 1964, doi: 10.1143/PTP.32.37.
- [15] A. Gómez *et al.*, "Assessment of the relationship between magnetotransport and magnetocaloric properties in nano-sized La0.7Ca0.3Mn1–xNixO3 manganites," *J. Magn. Magn. Mater.*, vol. 469, pp. 558–569, Jan. 2019, doi: 10.1016/j.jmmm.2018.09.036.